Published OnlineFirst November 9, 2010; DOI: 10.1158/0008-5472.CAN-10-0568

Cancer Research

Surface-Immobilized Aptamers for Cancer Cell Isolation and Microscopic Cytology

Yuan Wan[1,2], Young-tae Kim[1,2], Na Li[3], Steve K. Cho[4,5], Robert Bachoo[4,5,6], Andrew D. Ellington[3], and Samir M. Iqbal[2,7,8]

Abstract

Exposing rare but highly malignant tumor cells that migrate from the primary tumor mass into adjacent tissue(s) or circulate in the bloodstream is critical for early detection and effective intervention(s). Here, we report on an aptamer-based strategy directed against epidermal growth factor receptor (EGFR), the most common oncogene in glioblastoma (GBM), to detect these deadly tumor cells. GBMs are characterized by diffuse infiltration into normal brain regions, and the inability to detect GBM cells renders the disease surgically incurable with a median survival of just 14.2 months. To test the sensitivity and specificity of our platform, anti-EGFR RNA aptamers were immobilized on chemically modified glass surfaces. Cells tested included primary human GBM cells expressing high levels of the wild-type EGFR, as well as genetically engineered murine glioma cells overexpressing the most common EGFR mutant (EGFRvIII lacking exons 2–7) in Ink4a/Arf-deficient astrocytes. We found that surfaces functionalized with anti-EGFR aptamers could capture both the human and murine GBM cells with high sensitivity and specificity. Our findings show how novel aptamer substrates could be used to determine whether surgical resection margins are free of tumor cells, or more widely for detecting tumor cells circulating in peripheral blood to improve early detection and/or monitoring residual disease after treatment. *Cancer Res; 70(22); 9371–80. ©2010 AACR.*

Introduction

Early detection of cancer and its metastasis can dramatically change treatment and improve prognosis. There have been several approaches reported for the detection of tumor cells, including microfabricated devices that rely on mechanical forces (1, 2), dielectrophoresis (3), microscale optical interactions (4), immunohistochemistry (5, 6), magnetic cell sorting (7, 8), and flow cytometry (9). In contrast to mechanical and electrical sorting techniques, detection and sorting based on affinity interactions is expected to yield higher efficiency and greater specificity (10). Affinity-based approaches that rely on antibodies are often subject to high levels of off-target cross-reactivity (5, 11, 12). Moreover, there are considerable technical challenges to reproducibly cross-link antibodies to the surfaces of miniaturized devices due to heterogeneity of conjugation and surface denaturation.

There is increasing recognition that aptamers may have great utility in cancer diagnosis and therapeutics. Aptamers have been shown to have affinities and specificities that are comparable with those of antibodies, but have the advantage of being highly stable at a variety of salt and ionic conditions and can be reversibly denatured (13, 14). These can be chemically synthesized, site-specifically labeled, and therefore site-specifically immobilized. Moreover, because aptamers are much more hydrophilic than antibodies, they may provide surface passivation against nonspecific binding. Aptamers have been used in cell labeling studies (15, 16) as well as in activating cell signaling pathways (17–20). However, only recently, aptamers have been used in lab-on-chip devices to sort, isolate, and detect tumor cells (21). Here, we report results from an RNA aptamer substrate to isolate epidermal growth factor receptor (EGFR)–overexpressing primary human glioblastoma (hGBM) cells, as well as genetically engineered mouse glioma cells that photocopy human glioma. The approach provides a strong cytologic analysis modality to isolate and identify cancer cells. EGFR is the most frequently overexpressed receptor tyrosine kinase oncogene in all human malignancies that is activated on binding various growth factors and, in consequence, initiates a signal transduction cascade that promotes cell migration, adhesion, invasion, cell proliferation, angiogenesis, and antiapoptosis (22).

Authors' Affiliations: [1]Department of Bioengineering, [2]Nanotechnology Research and Teaching Facility, [3]Institute for Cell and Molecular Biology, University of Texas at Arlington, Arlington, Texas; [4]Internal Medicine, [5]Annette G. Strauss Center for Neuro-Oncology, and [6]Department of Neurology, University of Texas Southwestern Medical Center, Dallas, Texas; [7]Department of Electrical Engineering and [8]Joint Graduate Committee of Bioengineering Program, University of Texas at Arlington and University of Texas Southwestern Medical Center at Dallas, University of Texas at Arlington, Arlington, Texas

Note: Supplementary data for this article are available at Cancer Research Online (http://cancerres.aacrjournals.org/).

Current address for N. Li: AM Biotechnologies, LLC, Houston, TX 77034.

Current address for S.K. Cho: School of General Studies, GIST College, Gwangju Institute of Science and Technology, Gwangju, Korea.

Corresponding Author: Samir M. Iqbal, University of Texas at Arlington, 500 South Cooper Street, M.S. 19072, Room 217, Arlington, TX 76019. Phone: 817-272-0228; Fax: 817-272-7458; E-mail: smiqbal@uta.edu.

doi: 10.1158/0008-5472.CAN-10-0568

Published OnlineFirst November 9, 2010; DOI: 10.1158/0008-5472.CAN-10-0568

The overexpression of EGFR has been associated with several tumors, and EGFR is an attractive target for cancer therapy (23–25). The expression levels of EGFR vary from 40,000 to 100,000 proteins per cell in normal cells (26) and up to millions of proteins per cell in some tissue culture cell lines (27). The most common mutant of EGFR, EGFRvIII, results from a deletion of the extracellular amino acids 6 to 273 (exons 2–7), and this variant is expressed in glioma, non–small cell lung carcinomas, and breast carcinomas (28). Quantitative fluorescence-activated cell sorting analysis of human glioma biopsy-derived cells has shown that there are several hundred thousand EGFRvIII receptors per cell (28). Here, we present evidence that our surface-immobilized EGFR aptamers can be used to capture both primary hGBM cells expressing the endogenous wild-type EGFR as well as mutant EGFRvIII. The data presented here provide a proof-of-principle approach for identifying and isolating uniquely malignant subpopulations of tumor cells with a high degree of sensitivity and specificity.

Materials and Methods

All chemicals were obtained from Sigma-Aldrich unless otherwise noted.

Aptamer preparation

The anti-EGFR RNA aptamer was isolated by iteratively selecting binding species against purified human EGFR (R&D Systems) from a pool that spanned a 62-nucleotide random region (29). The EGFR protein was purified from murine myeloma cells and contained the extracellular domain of human EGFR (Leu^{25}-Ser^{645}) fused to the Fc domain of human IgG1 (Pro^{100}-Lys^{330}) via a peptide linker (IEGRMD). A high-affinity (K_d = 2.4 nmol/L) anti-EGFR aptamer and a nonfunctional, scrambled counterpart were extended with a capture sequence. The capture sequence did not disrupt aptamer structures but was used as a hybridization handle for binding with probes immobilized on surface.

The sequences for the extended anti-EGFR aptamer, mutant aptamer, and relevant capture oligonucleotides were as follows: anti-EGFR aptamer (5′-GGCGCUCCGACCUUAGUCUCUGUGCCGCUAUAAUGCACGGAUUUAAUCGCCGUAGAAAAGCAUGUCAAAGCCGGAACCGUGUAGCACAGCAGAGAAUUAAAUGCCCGCCAUGACCAG-3′), mutant aptamer (5′-GGCGCUCCGACCUUAGUCUCUGUUCCCACAUCAUGCACAAGGACAAUUCUGUGCAUCCAAGGAGGAGUUCUCGGAACCGUGUAGCACAGCAGAGAAUUAAAUGCCCGCCAUGACCAG-3′), and modified probe oligonucleotide (5′-amine-CTGGTCATGGCGGGCATTTAATTC-3′ or 5′-6FAM-CTGGTCATGGCGGGCATTTAATTC-3′). The capture sequence is underlined.

The anti-EGFR aptamer was prepared by transcribing a dsDNA template using Durascribe kits (Epicentre Biotechnologies). The DNA template was PCR amplified, ethanol precipitated, and mixed with reaction buffer, DTT, ATP, GTP, 2′ F-CTP, 2′ F-UTP, and a mutant T7 polymerase for 10 hours at 37°C. The DNA template was then degraded with DNase treatment for 30 minutes at 37°C. Aptamer was purified on an 8% denaturing PAGE. The band for the aptamer was visualized by UV shadowing, and the aptamer was excised and eluted in 0.3 mol/L sodium acetate (pH 5.2) overnight at 37°C followed by ethanol precipitation. The pellet was dissolved in water, and the concentration of aptamer was measured on a NanoDrop spectrophotometer (Thermo Scientific). The aptamer was modified by extending the DNA template at its 3′ end with a 24-nucleotide sequence tag, and then hybridizing the transcribed, extended aptamer with a cDNA oligonucleotide (referred to as probe oligonucleotide) labeled with 6-FAM or an amine at its 5′ end.

Preparation of anti-EGFR aptamer/antibody functionalized substrates

The attachment method was adapted from earlier descriptions (30, 31). The glass slides, used as substrates, were cut into 4 × 4 mm^2 pieces and cleaned in piranha solution (H_2O_2/H_2SO_4 in a 1:3 ratio) for 10 minutes at 90°C. After rinsing with deionized (DI) water and drying in nitrogen flow, the glass substrates were immersed in a 19:1 (v/v) methanol/DI water solution containing 3% APTMS for 30 minutes at room temperature. The silanized substrates were then sequentially rinsed with methanol and DI water and cured at 120°C for 30 minutes. The substrates were then immersed in a dimethylformamide (DMF) solution containing 10% pyridine and 1 mmol/L phenyldiisothiocyanate (PDITC) for 2 hours. Each substrate was then washed sequentially with DMF and 1,2-dichloroethane and dried under a stream of nitrogen. The DNA probes with an amine group modification at the 5′ end were prepared at 30 μmol/L concentration in DI water with 1% (v/v) *N*,*N*-diisopropylethylamine (DIPEA). A volume of 5 μL of DNA solution was placed on each substrate and allowed to incubate in a humidity chamber at 37°C overnight. Each substrate was then sequentially washed with methanol and diethyl pyrocarbonate (DEPC)–treated DI water (0.02%, v/v). The functionalized surface was then deactivated by capping unreacted PDITC moieties by immersion in 50 mmol/L 6-amino-1-hexanol and 150 mmol/L DIPEA in DMF for 5 hours. Each substrate was then sequentially rinsed with DMF, methanol, and DEPC-treated DI water. The incubator was cleaned with RNase-free and DEPC-treated DI water three times. A volume of 5 μL of anti-EGFR RNA aptamer at 1 μmol/L concentration was placed on each substrate in 1× annealing buffer [10 mmol/L Tris (pH 8.0), 1 mmol/L EDTA (pH 8.0), 100 mmol/L NaCl]. After 2 hours of hybridization at 37°C, substrates were washed with 1× annealing buffer and DEPC-treated DI water for 5 minutes. The negative control devices were hybridized with mutant aptamer using the same protocol. The substrates were placed in 1× PBS (pH 7.5) with 5 mmol/L magnesium chloride and kept at –20°C for 1 week or used immediately. The EGFR antibody attachment was adapted from previous reports (32, 33). A 100 μg/mL EGFR antibody solution was placed on the glass substrates and incubated at 37°C for 1 hour. Then, the substrates were blocked with bovine serum albumin (10 mg/mL) solution for 20 minutes, washed thoroughly with PBS, and placed in PBS solution.

Published OnlineFirst November 9, 2010; DOI: 10.1158/0008-5472.CAN-10-0568

Genetic engineering, isolation, and characterization of EGFR-overexpressed mouse-derived tumor cells (Ink4a/Arf$^{-/-}$ EGFRvIII neural stem cells)

Embryonic (E13.5) neural stem cells (NSC) were isolated from Ink4a/Arf$^{-/-}$ embryo brain, maintained under standard neurosphere culture conditions, and infected with a retrovirus expressing the mutant EGFRvIII receptor. The tumorigenicity of these cells has been extensively characterized by Bachoo and colleagues (34). The Ink4a/Arf$^{-/-}$ EGFRvIII NSCs were also stably transduced with a lentivirus expressing monomeric-cherry (referred to as *m-cherry*) fluorescent protein for live cell imaging and identification.

Isolation and characterization of hGBM cells

hGBM samples were obtained from consenting patients at the University of Texas Southwestern Medical Center (Dallas, TX) with the approval of the Institutional Review Board. On average, specimens >50 mm^3 were placed into ice-cold HBSS medium immediately on removal from the brain. Red blood cells were removed using lymphocyte-M (Cedarlane Labs). GBMs are highly cellular and molecularly heterogeneous tumors. Recent studies suggest that a minor cell population of GBM cells identified by a cell surface glycoprotein, CD133, may have an inexhaustible ability to self-renew, proliferate, and form a tumor when implanted into an immunocompromised host. GBM tumor cells that express CD133 have also been reported to be highly resistant to radiation and chemotherapy. While acknowledging the controversy of whether only CD133$^+$ cells are truly tumorigenic, for the purposes of this study, we used CD133$^+$ cells isolated from surgically resected samples that were also found to overexpress wild-type EGFR. The hGBM tumor tissue was gently dissociated with papain and dispase (both 2%), triturated, and then labeled with a CD133/2 (293C3)–PE antibody (Miltenyi Biotec) and sorted with FACSCalibur machine (BD Biosciences). Both CD133$^+$ and CD133$^-$ cells were suspended in a chemically defined serum-free DMEM/F-12 medium, consisting of 20 ng/mL of mouse EGF (PeproTech), 20 ng/mL of basic fibroblast growth factor (PeproTech), 1× B27 supplement (Invitrogen), 1× Insulin-Transferrin-Selenium-X (Invitrogen), and 100 units/mL penicillin–100 μg/mL streptomycin (HyClone), and plated at a density of 3 × 10^6 live cells/60-mm plate. Both CD133$^+$ and CD133$^-$ fractions underwent clonal expansion and formed orthotopic tumors (data not shown). For all the experiments, we used the CD133$^+$ fraction, referred to as hGBM cells. The hGBM cells were also stably transduced with a lentivirus expressing *m-cherry* fluorescent protein.

Meninge-derived primary fibroblast

Rat-derived primary meningeal fibroblasts were obtained from postnatal day 3 rat pups. Briefly, meninges were peeled from the cerebral cortices and then processed by incubation for 30 minutes in 0.5% collagenase and 20 minutes in 0.06% trypsin/EDTA, and then triturated. Following trituration, the cells were plated in T-75 tissue culture flasks in DMEM/F-12 medium containing 10% fetal bovine serum and allowed to grow for 1 week to confluence.

Results

Aptamer binding to cultured tumor cells

To show the selective binding of aptamer to tumor cells, the anti-EGFR aptamer, annealed with 6-FAM–modified capture oligonucleotide, was incubated with tumor cells and fibroblasts, and interaction was measured as follows: The DNA probe labeled with 6-FAM was used as received (Alpha DNA). Equal amounts of anti-EGFR RNA aptamer and DNA capture probe were annealed by heating samples to 70°C for 10 minutes and then slowly cooling to room temperature. Both mouse-derived tumor cells and primary fibroblasts were seeded into separate PDMS wells (8-mm diameter) and cultured for 48 hours. The RNA/DNA capture probe was incubated with cells at 37°C for 30 minutes under 5% CO_2. After incubation, the cells were washed with 1× PBS three times and stored in freshly sterilized 1× PBS for differential interference contrast (DIC) and fluorescence imaging. DIC data were used to image the cells, and fluorescence imaging was focused on aptamers. Mutant aptamer was also applied into the cells as a control, and all experimental procedures were the same as those for the anti-EGFR aptamer. The fluorescence images were taken using appropriate filters. The excitation and emission wavelength of 6-FAM are 492 and 517 nm, respectively.

Tumor cell capture using anti-EGFR aptamer/antibody substrates

In all experiments, the cells were centrifuged and the supernatants were removed. Sterilized 1× PBS solution (with 5 mmol/L $MgCl_2$) was added to dilute the centrifuged cells. About 50 μL of cell suspension were placed on each substrate. The substrates were incubated for 30, 60, or 90 minutes at 37°C (15) and then washed with PBS solution on a shaker (Boekel Scientific) at 90 rpm for 6 to 10 minutes in orbital and reciprocal movements. The time of incubation was also studied for saturation effects. There was no difference seen in the results for the three different groups of 30-, 60-, and 90-minute incubation. The buffer evaporation was seen for longer incubation. The subsequent incubations of cells were thus done for 30 minutes. For tumor-specific isolation studies, the hGBM cells were mixed with fibroblasts in a 1:1 ratio. Mutant aptamer-functionalized substrates were used as controls. The experiments of EGFR capture with antibodies followed exactly the same procedure.

Monitoring of the dynamic interactions between the tumor cells and the anti-EGFR aptamer-functionalized substrates

To visualize tumor cell capture via the anti-EGFR aptamer substrates, these were placed on a custom-designed neuro-optical microfluidic platform, and the interaction between tumor cells and surface-grafted aptamers was monitored as described previously (35). Briefly, the substrates were placed on the platform, which maintained 5% CO_2 at 37°C and high humidity for live cell imaging. The interactions between cells

Published OnlineFirst November 9, 2010; DOI: 10.1158/0008-5472.CAN-10-0568

and anti-EGFR aptamer surfaces were closely monitored using an inverted microscope (63×: DIC). Images were taken every 30 seconds, and the interaction was recorded for 30 minutes. The tumor cells were also seeded on the control substrates (with mutant aptamer), and the interaction was closely monitored in a similar manner.

Quantification and statistical analysis

For analysis, 5 representative images (of 25 total substrate areas) were randomly taken from each substrate. The images were analyzed with Image-Pro Plus software. The total number of captured cells and their relevant diameters on the surface were counted automatically, and the cell densities (number of cells per mm^2) were calculated. To show the diameter of tumor cells on aptamer-grafted substrates, the data were sorted into six groups based on cell sizes (from 20 μm to the maximum; 5-μm interval), and relevant percentages were obtained.

Discussion

The use of microfluidic devices to isolate rare tumor cells is of great importance. The capture of tumor cells requires the affinity recognition of specific biomarkers. The challenge is to efficiently isolate a small number of tumor cells from a much larger pool of normal cells (5). Aptamers may prove to be uniquely useful for lab-on-chip devices because of their high and specific affinities for analytes, and the versatility of conjugation and labeling inherent in their chemical synthesis. Before we used the RNA aptamer substrates to identify and isolate EGFR-overexpressed cancer cells, we confirmed the specific binding between mouse-derived glioma cells and the anti-EGFR aptamers.

Aptamer binding to mouse-derived tumor cells

The probe oligonucleotides modified with 6-FAM dye were hybridized to the anti-EGFR and mutant (as control) aptamers, and specific binding to cultured mouse-derived glioma cells was observed (Fig. 1). An additional control for specificity was to incubate the anti-EGFR aptamer with a noncognate cell, primary fibroblasts. After washing, green fluorescence was observed only with the mouse-derived tumor cell surface incubated with the labeled anti-EGFR aptamers (Fig. 1B). The controls included (*a*) mutant aptamer incubated with mouse-derived glioma cells, (*b*) anti-EGFR aptamer with fibroblast, and (*c*) mutant aptamer with fibroblasts. The fluorescence intensity data are shown in Fig. 1C. Similar results were obtained for hGBM cells. This showed the specific binding of anti-EGFR aptamer with tumor cells. These mouse-derived tumor cells and primary hGBM cells express the endogenous wild-type EGFR as well as mutant EGFRvIII, but the expression level of wild-type EGFR on mouse-derived tumor cells is much lower. Because the aptamer is also known to compete with EGF for binding, these results are consistent with the aptamer binding to the ligand-binding domain III of the extracellular region, which falls outside of the deletion encompassed by exons 2 to 7 in EGFRvIII.

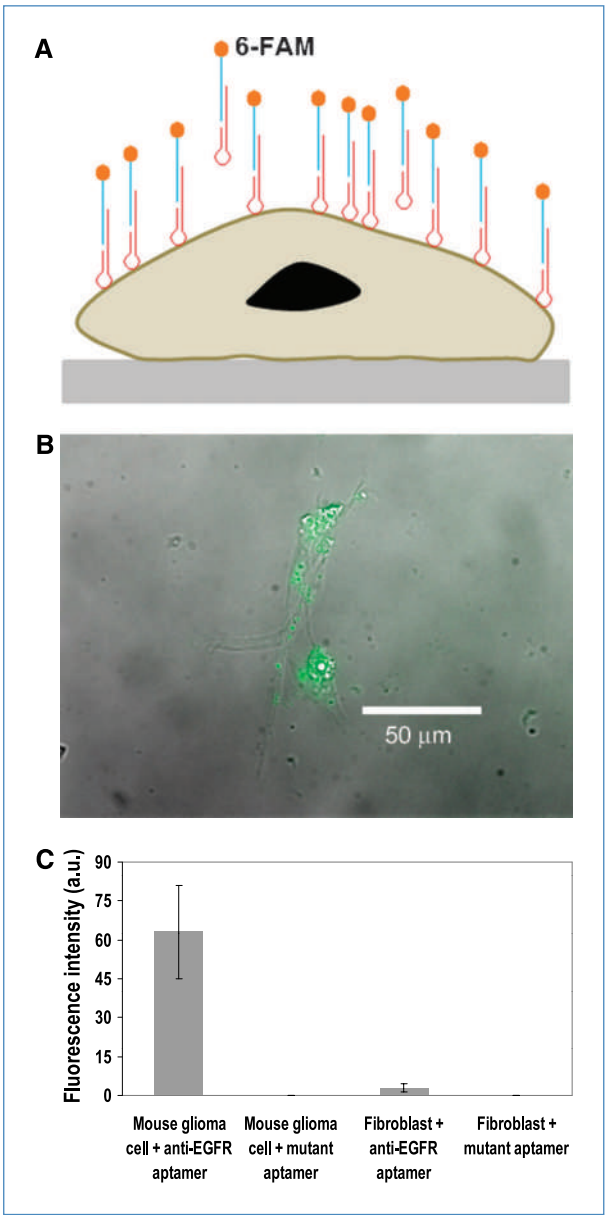

Figure 1. Anti-EGFR aptamer binding to the cultured mouse-derived tumor cell. The RNA aptamer was annealed to 6-FAM–modified DNA probe. The RNA aptamer–DNA probe complex was allowed to interact and bind to mouse-derived tumor cells at 37°C for 30 min in 5% CO_2. After binding, the cells were washed with 1× PBS three times. A, schematic depicting mouse-derived cell bound with aptamer complex. B, overlaid fluorescent and DIC images. The green fluorescent shows the cell-bound aptamer molecules; the excitation and emission wavelength of 6-FAM are 492 and 517 nm, respectively. C, average fluorescence intensity of each group.

Capture and morphologic characteristics of mouse-derived tumor cells overexpressing EGFR

The functionalization of the substrates yielded a homobifunctional layer of PDITC that can be used to immobilize any amine-modified molecules. An amine-bearing capture oligonucleotide was conjugated to the surface, which in turn

Published OnlineFirst November 9, 2010; DOI: 10.1158/0008-5472.CAN-10-0568

allowed the capture of the extended aptamer. The capping of unreacted PDITC end groups ensured that nonspecific adsorption of aptamer did not occur. The use of probe oligonucleotides for the functionalization of the substrates has many advantages: it shows a generalized approach to capture any functional nucleic acid, a distinct advantage relative to the use of proteins; it increases the distance between the substrate surface and the aptamer, alleviating the effects of steric and/or electrostatic hindrance that may come from surface tethering; and it increases the radius of gyration of the aptamer, thereby potentially increasing reactivity. This also resulted into very distinct behavior of cells when interacting with aptamers (discussed later).

Genetically engineered mouse glioma cells were incubated on the aptamer substrates and washed with warmed 1× PBS (Fig. 2; ref. 36). A significantly higher number of the mouse-derived EGFR-overexpressed tumor cells were seen bound to the anti-EGFR aptamer-functionalized surfaces (Fig. 3), with an isolation efficiency (the ratio of captured cell number to the original number of cells on the surface) of 62.32%. A very small number of cells (average 7 cells/mm^2) were captured on the mutant aptamer-functionalized control substrates.

These results may reveal an additional important feature of the use of nucleic acids on possible lab-on-chip devices. Nucleic acids may provide a passivation layer that minimizes nonspecific adsorption. The hydrophilic surface and electrostatic repulsion may have prevented any nonselective physical adsorption of the cells on mutant aptamer substrates (37–39). The density and amount of sialylation on the surface of cancer cells is higher than on normal ones (40–42). Carboxyl groups from sialic acid cause a net negative surface charge on cancer cells. The repulsion between negatively charged cells and the negative charges from the surface-functionalized aptamer can be another putative reason for the lack of nonspecific adsorption. On the other hand, the cancer cells that could selectively interact and bind to the aptamer got captured on the surface, even in the presence of above-stated competing forces. The use of capture oligonucleotides thus has the advantage of reducing nonspecific binding or adsorption, adding to the selectivity of the substrates. The use of probe DNA to covalently immobilize aptamers thus provides a robust passivation of the surface that provides functionality and selectivity with screening effects of surface charges.

The density and diameters of captured cells showed distinct behavior on the anti-EGFR and mutant aptamer substrates (Fig. 3B). On average, there were ~392 cancer cells captured per mm^2 on 12 anti-EGFR aptamer substrates (SD, 143.3), with the size ranges depicted in the figure. Interestingly, ~70% of the captured cells had diameters above 30 μm, whereas the size of these cells in suspension ranged between 25 and 30 μm. This indicates that cancer cells were spreading on the anti-EGFR aptamer substrates. Although there are reports that show size differences of normal cells and cancer cells as discriminating factor, there is still not conclusive evidence that cancer cells are bigger than the normal cells. In any case, the new class of binding between anti-EGFR aptamer substrates and EGFR-expressing cells is an important analytic tool, serving as a novel and important phenomenon that can be a discriminating factor in cytologic studies for the confirmation of the captured tumor cells.

Capture of hGBM cells

EGFR expression level on hGBM cells was ~50% compared with the genetically engineered mouse glioma cells

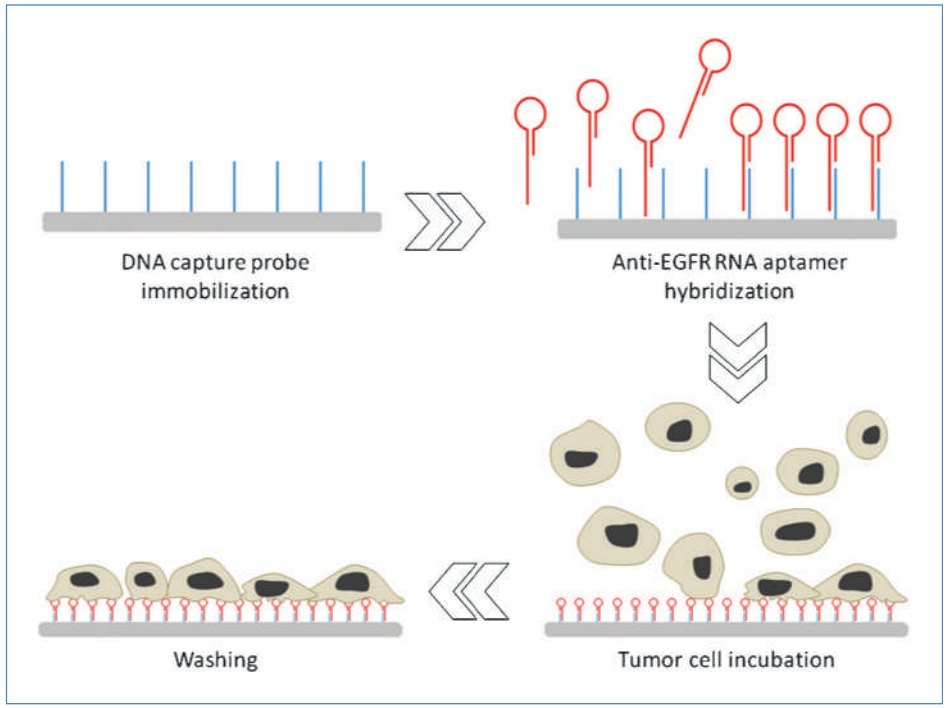

Figure 2. Schematics showing steps of experiments (not drawn to scale). The amine-modified DNA probes were first immobilized on the glass substrates. After hybridization with 1 μmol/L anti-EGFR RNA aptamer at 37°C for 2 h, substrates were incubated with tumor cells at 37°C for 30 min. After incubation, the substrates were washed with 1× PBS for 8 min.

Published OnlineFirst November 9, 2010; DOI: 10.1158/0008-5472.CAN-10-0568

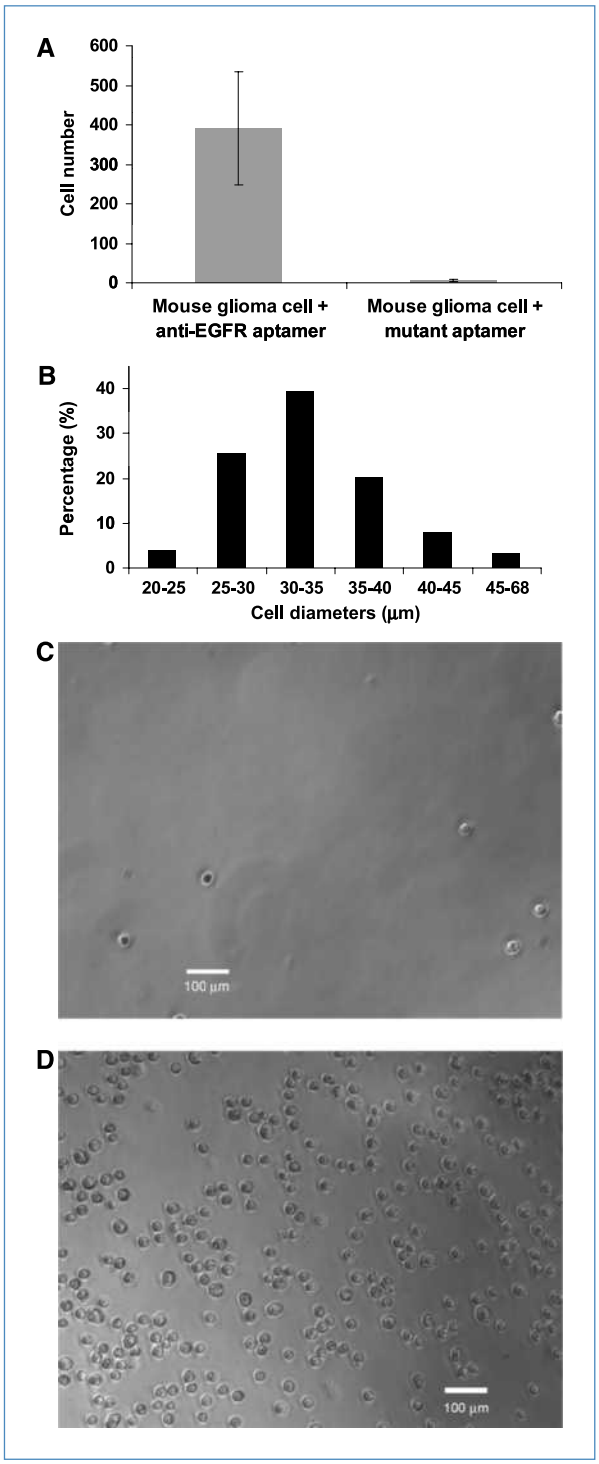

Figure 3. The density and size ranges of captured cells. Substrates were incubated with mouse-derived tumor cells and washed with 1× PBS. A, average tumor cell density on 12 anti-EGFR aptamer substrates (average, 392 cells per mm^2; max, 831 cells per mm^2; min, 284 cells per mm^2; SD, 143.3) and on 12 control substrates with mutant aptamer (average, 7 cells per mm^2; max, 11 cells per mm^2; min, 0 cells per mm^2; SD, 2.8). *, $P < 0.01$. B, distribution of the diameters of tumor cells on 12 anti-EGFR aptamer substrates. C and D, representative pictures of tumor cells on (C) mutant aptamer and (D) anti-EGFR aptamer-grafted surfaces.

(level verified by Western blot; data not shown). Despite the relatively lower EGFR expression level, hGBM cells were captured with comparable sensitivity and specificity by the anti-EGFR aptamer–functionalized substrates. These cells did not bind to mutant aptamer control substrates (Fig. 4).

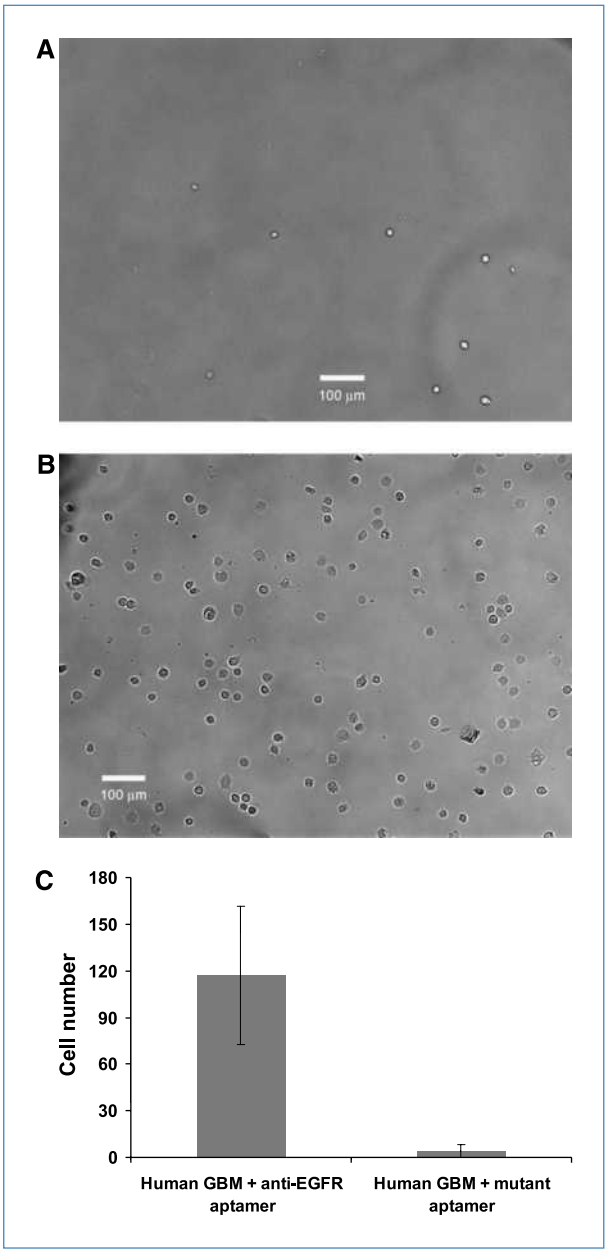

Figure 4. The hGBM cells on the substrates. Substrates were incubated with hGBM and washed with PBS. The hGBM cells captured on (A) the mutant aptamer control substrate and (B) the anti-EGFR aptamer substrate. C, average hGBM cell density on 12 anti-EGFR aptamer substrates (average, 117 cells per mm^2; max, 228 cells per mm^2; min, 56 cells per mm^2; SD, 44.4) and on 12 control substrates with mutant aptamer (average, 4 cells per mm^2; max, 13 cells per mm^2; min, 0 cells per mm^2; SD, 4.1). *, $P < 0.01$.

Published OnlineFirst November 9, 2010; DOI: 10.1158/0008-5472.CAN-10-0568

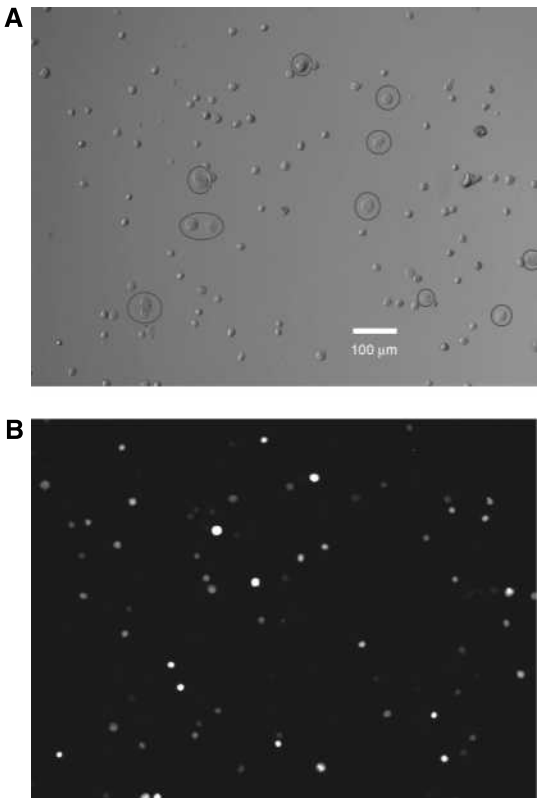

Figure 5. The hGBM and fibroblast cells on the substrate surfaces. Substrates were incubated with mixture of hGBM and fibroblast and washed with PBS. A and B, DIC and fluorescent images, respectively, from the same position. The circles in A indicate a few fibroblasts that were captured and cannot be seen in B.

Figure 4 shows the clear difference in the number and cell shapes of hGBM cells on anti-EGFR and mutant aptamer substrates. Along with difference in the numbers of captured cells, the shapes of the cells bound with aptamers and adsorbed on mutant aptamer surfaces were also quite different (discussed later). Analysis of 12 substrates showed that on average 117 hGBM cells were captured per mm^2 on anti-EGFR aptamer substrate (SD, 44.4; max and min of 228 and 56 cells per mm^2, respectively), with isolation efficiency of 38.74%. In the control mutant substrate group, average density of 4 cells per mm^2 was seen (SD, 3.1; max and min densities of 13 and 0 cells per mm^2, respectively). In comparison with the mouse-derived tumor cells, a smaller number of captured hGBM cells than that for mouse-derived tumor cells (discussed in previous section) can be explained in terms of an overly high number of EGFR that were genetically engineered in mouse-derived tumor cells. The decreased density of captured hGBM cells was thus as expected.

Isolation of cancer cells from cell mixture

In the above two experiments (mouse-derived tumor cells and primary hGBM cells), we confirmed that the anti-EGFR aptamer-functionalized substrates could capture significantly more tumor cells compared with that of the mutant aptamer. Toward the application of aptamer-functionalized substrates in isolating tumor cells and to study their behavior, a cell mixture was used. A mixture of hGBM and fibroblast cells was prepared in a ratio of 1:1, and the average cell density on the surface was 303 per mm^2 (SD, 11.95). The substrates were incubated in the mixture and washed, and the results were imaged. In parallel experiments, only hGBM cells were incubated with substrates. Both DIC and fluorescent images were taken (Fig. 5A and B). In hGBM-only surfaces, the fluorescent intensities were not uniform when DIC and fluorescent images were overlaid (hGBM cells were modified to express m-cherry fluorescent protein for clear differentiation). There were ~16.7% cells from 12 substrates that did not show any fluorescence (189 of 1,133 cells from 12 substrates; average, 16; SD, 5.1). The data from the mixture group showed no fluorescence from ~27.5% cells from 12 substrates (378 of 1,376 cells from 12 substrates; average, 31.5; SD, 6.8). The cells that did not show up in fluorescence images included captured hGBM and nonspecifically bound fibroblast cells. The difference of the two percentages, as a first-order approximation, shows that on average ~10.8% captured cells were fibroblasts. Thus, the anti-EGFR aptamer substrates can selectively isolate and enrich a 1:1 mixture suspension ratio of fibroblasts to cancer cells, to 1:8.24 on the surface. In the EGFR antibody substrate control group,

Table 1. Comparison between capture efficiency of anti-EGFR aptamer and EGFR-specific antibody

	EGFR antibody		Anti-EGFR aptamer	
	hGBM cells	Fibroblast	hGBM cells	Fibroblast
Captured	188	68	84	10
Uncaptured	30	150	134	208

NOTE: The average number of cells on 10 substrate surfaces is 436 (5 with EGFR antibody and 5 with anti-EGFR aptamer). Because the hGBMs were mixed with fibroblast in the ratio of 1:1, 218 hGBMs and 218 fibroblast cells were considered for this comparison. The average captured hGBMs and fibroblasts on EGFR antibody substrates are 188 (SD, 17.2) and 68 (SD, 11.0), respectively, and the average captured hGBMs and fibroblasts on anti-EGFR aptamer substrates are 84 (SD, 22.8) and 10 (SD, 4.3), respectively.

Published OnlineFirst November 9, 2010; DOI: 10.1158/0008-5472.CAN-10-0568

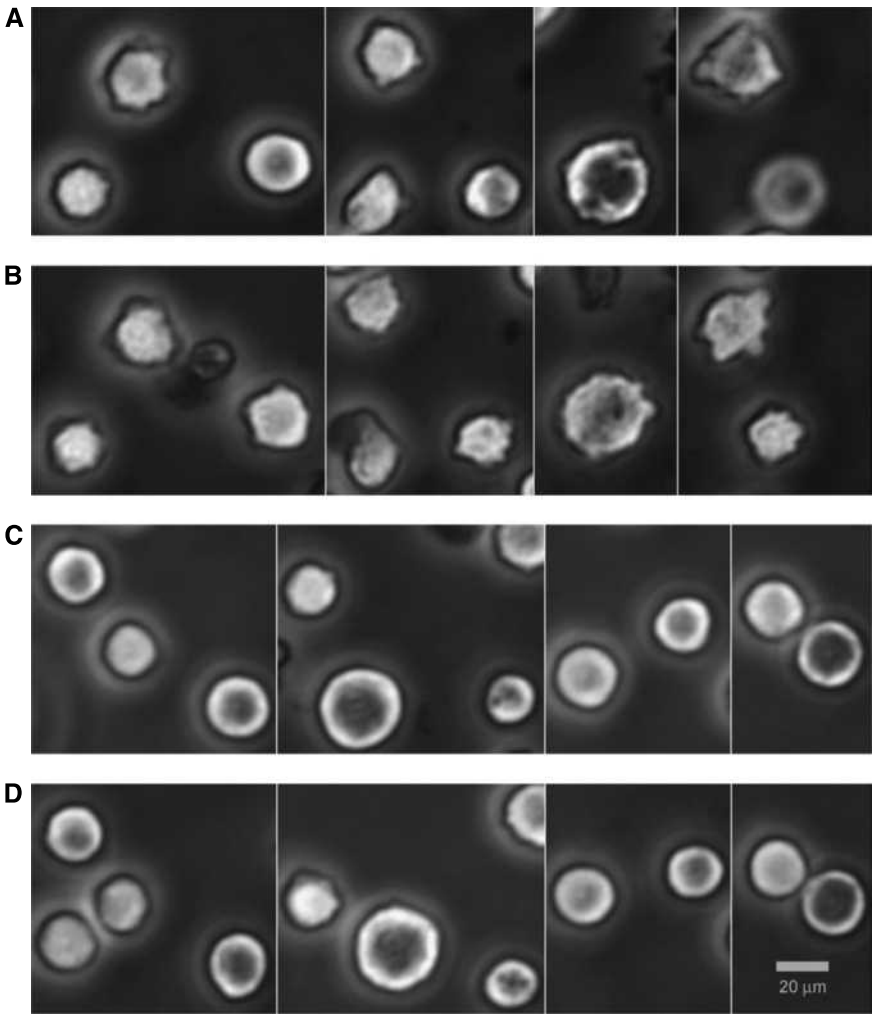

Figure 6. The changes in shapes of mouse-derived tumor cells. A and C, taken 3 min after seeding the cells on the anti-EGFR and mutant aptamer substrates, respectively. B and D, taken 30 min later on the anti-EGFR and mutant aptamer substrates, respectively. A and B, changes of cell shapes on the anti-EGFR aptamer-grafted surface in 30 min. C and D, no changes in cell shapes on mutant aptamer substrates.

the ratio of captured fibroblasts to cancer cells was 1:2.77. The specificity of aptamer and antibody on cancer cell isolation was thus 94.82% and 68.81%, respectively (Table 1). The results show that aptamer has higher specificity. In a practical scenario, as a lower limit, the aptamer-grafted substrates can enrich the amount of cancer cells by an order from the concentration in the solution. In a cyclic iteration application, a sample can be run for multiple times over the substrates to increase the capture efficiency. It may be important to note here that "mean capture yield" using anti-EpCAM antibodies has been shown to be ~65% (5). Further studies are under way to verify this efficiency with varying ratios of tumor cells and cancer xenografts.

Shape and size of cancer cells on functionalized substrates

In all the experiments, the cell shapes and sizes showed a distinct behavior: fibroblasts altered their fusiform, stellar, or irregular shape to spherical. Mouse fibroblasts showed low levels of wild-type EGFR expression on their cell membrane, far less than primary hGBM cells or the mouse-derived glioma cells. To bind with anti-EGFR aptamer, the cells altered their shape to decrease their surface area to increase the EGFR density that would come in contact with the surface-bound aptamer. The temporal images of mouse-derived tumor cells also showed changes in cell shapes from spherical in suspension to semi-elliptic and flat on the aptamer-grafted surfaces (Fig. 6). The different cell behavior on the surface may be a result of different elasticity in cancer cells (43). The EGFR-overexpressed cells were reshaping to cover as large of an area as possible. Temporal imaging also showed tumor cell migration on surfaces. The images for Fig. 6A and C were taken at the beginning when mouse-derived tumor cells were seeded on the anti-EGFR and mutant aptamer surfaces, and the images for Fig. 6B and D were taken after 30 minutes. Changes in cells shapes and flatness are evident in going from Fig. 6A to B only. The size of cells also became bigger, and many pseudopodia formed during the incubation period on anti-EGFR aptamer substrates (Supplementary Video S1). The video also shows that the

Published OnlineFirst November 9, 2010; DOI: 10.1158/0008-5472.CAN-10-0568

tumor cells on the substrate surface had strong activity and were arbitrarily changing their shape. In contrast, going from Fig. 6C to D, first, only much fewer cells did get capture on the mutant aptamer surfaces, and second, those too faced repulsion from the hydrophilic glass surface and the negative charges from the immobilized oligonucleotides. Consequently, the cells had almost no change in their sizes during the 30 minutes. The data on hGBM cell shapes in Fig. 4A also show that cells on mutant aptamer substrates maintained globular shape as discussed above. The spreading and flatness of cancer cells on aptamer surfaces can be an important modality for detection as an additional method to support histologic findings and further identify tumor cells based on their physical behaviors. In addition, hGBM cells are diffusively infiltrative and current methods to define tumor margins for surgical resection, using magnetic resonance imaging, are inadequate. Histologic evidence suggests that tumor cells at the leading edge may express high levels of EGFR. It is possible, therefore, that freshly resected tumor could be enzymatically dissociated and captured on the anti-EGFR aptamer-functionalized substrates, in real time, to better define tumor margins. Such information, thus, can help guide the extent of tumor resection as well. There is considerable evidence that the extent of resection is directly related to overall survival. Beyond the specific application for management of hGBM tumors, our findings are especially important given that enrichment of rare circulating tumor cells may be difficult for virtually any lab-on-chip device. The use of aptamers leads both to high passivation and the presentation of unique physical morphologies, and thus may be a novel first-level detection step in point-of-care examination of circulating tumor cells.

Conclusions

It has been shown that anti-EGFR RNA aptamer substrates can specifically recognize, capture, and isolate cancer cells that are known to overexpress EGFR. The aptamers can capture both human and murine GBM cells expressing wild-type EGFR and mutant EGFRvIII with high sensitivity and specificity. Aptamer substrates also specifically isolated hGBM cells from a mixture of fibroblasts. The isolation efficiency depended on strong binding between aptamer and the amount of EGFR expression on the cell membrane. The change in cell shape and cellular activity can serve as a novel way of identifying tumor cells. The substrates can also be used for identification and isolation of circulating tumor cells from peripheral blood, dramatically changing intervention and prognosis of metastasis.

Disclosure of Potential Conflicts of Interest

No potential conflicts of interest were disclosed.

Acknowledgments

We thank Charles Huang, Priyanka P. Ramachandran, and Swati Goyal for help with experimental setup; Waseem Asghar and Melissa Johnson for help with manuscript preparation; Kailash Karthikeyan for help with video capturing; and staff of Nanotechnology Research and Teaching Facility for equipment training.

Grant Support

The work at the University of Texas at Arlington was supported with NSF CAREER grant ECCS-0845669 (S.M. Iqbal). The work at the University of Texas at Austin was supported by Welch Foundation grant F-1654 and National Cancer Institute Award Number 5R01CA119388-05.

The costs of publication of this article were defrayed in part by the payment of page charges. This article must therefore be hereby marked *advertisement* in accordance with 18 U.S.C. Section 1734 solely to indicate this fact.

Received 02/17/2010; revised 08/24/2010; accepted 09/14/2010; published OnlineFirst 11/09/2010.

References

1. Mohamed H, McCurdy LD, Szarowski DH, et al. Development of a rare cell fractionation device: application for cancer detection. IEEE Trans Nanobioscience 2004;3:251–6.
2. Huang LR, Cox EC, Austin RH, et al. Continuous particle separation through deterministic lateral displacement. Science 2004;304:987–90.
3. Bustin SA, Gyselman VG, Siddiqi S, et al. Cytokeratin 20 is not a tissue-specific marker for the detection of malignant epithelial cells in the blood of colorectal cancer patients. Int J Surg Invest 2000;2:49–57.
4. MacDonald MP, Neale S, Paterson L, et al. Cell cytometry with a light touch: sorting microscopic matter with an optical lattice. J Biol Regul Homeostatic Agents 2004;18:200–5.
5. Nagrath S, Sequist LV, Maheswaran S, et al. Isolation of rare circulating tumour cells in cancer patients by microchip technology. Nature 2007;450:1235–9.
6. Feng J, Soper SA, McCarley RL, et al. Separation of breast cancer cells from peripherally circulating blood using antibodies fixed in microchannels. Proc SPIE 2004;5312:278–93.
7. Tibbe AG, de Grooth BG, Greve J, et al. Magnetic field design for selecting and aligning immunomagnetic labeled cells. Cytometry 2002;47:163–72.
8. Lee H, Sun E, Ham D, et al. Chip-NMR biosensor for detection and molecular analysis of cells. Nat Med 2008;14:869–74.
9. He W, Wang H, Hartmann LC, et al. *In vivo* quantitation of rare circulating tumor cells by multiphoton intravital flow cytometry. Proc Natl Acad Sci U S A 2007;104:11760–5.
10. Toner M, Irimia D. Blood-on-a-chip. Annu Rev Biomed Eng 2005;7:77–103.
11. Baas IO, van den Berg FM, Mulder JW, et al. Potential false-positive results with antigen enhancement for immunohistochemistry of the p53 gene product in colorectal neoplasms. J Pathol 1996;178:264–7.
12. Dalle F, Lopez J, Caillot D, et al. False-positive results caused by cotton swabs in commercial *Aspergillus* antigen latex agglutination test. Eur J Clin Microbiol Infect Dis 2002;21:130–2.
13. Bunka DH, Stockley PG. Aptamers come of age—at last. Nat Rev Microbiol 2006;4:588–96.
14. Sullenger BA, Gilboa E. Emerging clinical applications of RNA. Nature 2002;418:252–8.
15. Farokhzad OC, Jon S, Khademhosseini A, et al. Nanoparticle-aptamer bioconjugates: a new approach for targeting prostate cancer cells. Cancer Res 2004;64:7668–72.
16. Chen HW, Medley CD, Sefah K, et al. Molecular recognition of

Published OnlineFirst November 9, 2010; DOI: 10.1158/0008-5472.CAN-10-0568

small-cell lung cancer cells using aptamers. ChemMedChem 2008;3:991–1001.
17. Nagel-Wolfrum K, Buerger C, Wittig I, et al. The interaction of specific peptide aptamers with the DNA binding domain and the dimerization domain of the transcription factor Stat3 inhibits transactivation and induces apoptosis in tumor cells. Mol Cancer Res 2004;2:170–82.
18. Usman N, Blatt LM. Nuclease-resistant synthetic ribozymes: developing a new class of therapeutics. J Clin Invest 2000;106:1197–202.
19. Charlton J, Sennello J, Smith D. *In vivo* imaging of inflammation using an aptamer inhibitor of human neutrophil elastase. Chem Biol 1997;4:809–16.
20. Bates PJ, Laber DA, Miller DM, et al. Discovery and development of the G-rich oligonucleotide AS1411 as a novel treatment for cancer. Exp Mol Pathol 2009;86:151–64.
21. Phillips JA, Xu Y, Xia Z, et al. Enrichment of cancer cells using aptamers immobilized on a microfluidic channel. Anal Chem 2008;81:1033–9.
22. Mendelsohn J. EGF receptors as a target for cancer therapy. Trans Am Clin Climatol Assoc 2004;115:249–53.
23. Franovic A, Gunaratnam L, Smith K, et al. Translational up-regulation of the EGFR by tumor hypoxia provides a nonmutational explanation for its overexpression in human cancer. Proc Natl Acad Sci U S A 2007;104:13092–7.
24. Maheswaran S, Sequist LV, Nagrath S, et al. Detection of mutations in EGFR in circulating lung-cancer cells. N Eng J Med 2008;359:366–77.
25. Chakravarti A, Loeffler JS, Dyson NJ. Insulin-like growth factor receptor I mediates resistance to anti-epidermal growth factor receptor therapy in primary human glioblastoma cells through continued activation of phosphoinositide 3-kinase signaling. Cancer Res 2002;62:200–7.
26. Carpenter G, Cohen S. Epidermal growth factor. Annu Rev Biochem 1979;48:193–216.
27. Carpenter G. The biochemistry and physiology of the receptor-kinase for epidermal growth factor. Mol Cell Endocrinol 1983;31:1–19.
28. Wikstrand CJ, McLendon RE, Friedman AH, et al. Cell surface localization and density of the tumor-associated variant of the epidermal growth factor receptor, EGFRvIII. Cancer Res 1997;57:4130–40.
29. Osborne SE, Matsumura I, Ellington AD. Aptamers as therapeutic and diagnostic reagents: problems and prospects. Curr Opin Chem Biol 1997;1:5–9.
30. Möller R, Csáki A, Köhler JM, et al. DNA probes on chip surfaces studied by scanning force microscopy using specific binding of colloidal gold. Nucleic Acids Res 2000;28:e91.
31. Iqbal SM, Akin D, Bashir R. Solid-state nanopore channels with DNA selectivity. Nat Nanotechnol 2007;2:243–8.
32. Mezzasoma L, Bacarese-Hamilton T, Di Cristina M, et al. Antigen microarrays for serodiagnosis of infectious diseases. Clin Chem 2002;48:121–30.
33. Raj J, Herzog G, Manning M, et al. Surface immobilisation of antibody on cyclic olefin copolymer for sandwich immunoassay. Biosens Bioelectron 2009;24:2654–8.
34. Bachoo RM, Maher EA, Ligon KL, et al. Epidermal growth factor receptor and Ink4a/Arf Convergent mechanisms governing terminal differentiation and transformation along the neural stem cell to astrocyte axis. Cancer Cell 2002;1:269–77.
35. Kim Y, Karthikeyan K, Chirvi S, et al. Neuro-optical microfluidic platform to study injury and regeneration of single axons. Lab Chip 2009;9:2576–81.
36. Cheung LSL, Zheng X, Stopa A, et al. Detachment of captured cancer cells under flow acceleration in a bio-functionalized microchannel. Lab Chip 2009;9:1721–31.
37. Morisaki H. A novel system for the analysis of cell attachment in *Pseudomonas syringae*. J Microbiol Methods 1995;22:69–78.
38. Hazen KC, Brawner DL, Riesselman MH, et al. Differential adherence between hydrophobic and hydrophilic yeast cells of *Candida albicans*. Infect Immun 1991;59:907–12.
39. Tamada Y, Ikada Y. Effect of preadsorbed proteins on cell adhesion to polymer surfaces. J Colloid Interface Sci 1993;155:334–9.
40. Kokoglulu E, Sonmez H, Uslu E, et al. Sialic acid levels in various types of cancer. Cancer Biochem Biophys 1992;13:57–64.
41. Khadapkar SV, Sheth NA, Bhide SV. Independence of sialic acid levels in normal and malignant growth. Cancer Res 1975;35:1520–3.
42. Sillanaukee P, Pönniö M, Jääskeläinen IP. Occurrence of sialic acids in healthy humans and different disorders. Eur J Clin Invest 1999;29:413–25.
43. Lekka M, Laidler P, Ignacak J, et al. The effect of chitosan on stiffness and glycolytic activity of human bladder cells. Biochim Biophys Acta 2001;1540:127–36.

Cancer Research

Correction: Surface-Immobilized Aptamers for Cancer Cell Isolation and Microscopic Cytology

In this article (Cancer Res 2010:70;9371–80), which was published in the November 15, 2010 issue of *Cancer Research* (1), several of the author affiliations were incorrect. The correct affiliations are provided below.

Yuan Wan[1,2], Young-tae Kim[1,2], Na Li[3], Steve K. Cho[4,5], Robert Bachoo[4–6], Andrew D. Ellington[3], and Samir M. Iqbal[2,7,8]

[1]Department of Bioengineering, [2]Nanotechnology Research and Teaching Facility, University of Texas at Arlington, Arlington; [3]Institute for Cell and Molecular Biology, University of Texas at Austin, Austin; [4]Internal Medicine, [5]Annette G. Strauss Center for Neuro-Oncology; [6]Department of Neurology, University of Texas Southwestern Medical Center, Dallas; [7]Department of Electrical Engineering, [8]Joint Graduate Committee of Bioengineering Program, University of Texas at Arlington, and University of Texas Southwestern Medical Center at Dallas, University of Texas at Arlington, Arlington, Texas

Reference

1. Wan Y, Kim Y, Li N, Cho SK, Bachoo R, Ellington AD, et al. Surface-immobilized aptamers for cancer cell isolation and microscopic cytology. Cancer Res 2010:70;9371–80.

Published OnlineFirst January 11, 2011

doi: 10.1158/0008-5472.CAN-10-4187

Cancer Research
The Journal of Cancer Research (1916–1930) | The American Journal of Cancer (1931–1940)

AACR American Association for Cancer Research

Surface-Immobilized Aptamers for Cancer Cell Isolation and Microscopic Cytology

Yuan Wan, Young-tae Kim, Na Li, et al.

Cancer Res 2010;70:9371-9380. Published OnlineFirst November 9, 2010.